Structures 70 (2024) 107838

Contents lists available at ScienceDirect

Structures

journal homepage: www.elsevier.com/locate/structures

Mechanical behavior of composite slabs with recycled concrete aggregates: A preliminary study

Flavio Stochino [a,*], Alireza Alibeigibeni [a], Marco Zucca [a], Monica Valdes [a], Giovanna Concu [a], Marco Simoncelli [b], Marco Andrea Pisani [b], Claudio Bernuzzi [b]

[a] Department of Civil Environmental Engineering and Architecture, University of Cagliari, via Marengo 2, 09123 Cagliari, CA, Italy
[b] Department of Architecture, Built Environment and Construction Engineering, Politecnico di Milano, Via G. Ponzio 31, 20133 Milano, MI, Italy

ARTICLE INFO

Keywords:
Sustainability
Concrete
Composite structures
Composite slabs
Recycled aggregate
Construction and demolition waste

ABSTRACT

The imperative to mitigate the environmental footprint of concrete structures is increasingly recognized in scientific and engineering spheres. Of particular concern is the escalating demand for natural aggregates, which prompts the establishment of new quarries, thereby exacerbating environmental concerns. A viable remedy to this challenge lies in the utilization of recycled aggregates sourced from construction and demolition waste in concrete production. Concurrently, composite slabs offer a host of advantages over conventional reinforced concrete counterparts. These benefits encompass heightened strength and stiffness, expedited and simplified installation processes, and diminished environmental repercussions. Consequently, the incorporation of recycled aggregates in composite slabs emerges as a promising strategy for environmental sustainability within the realm of concrete construction. This experimental study investigates the mechanical behavior of composite slabs incorporating Recycled Concrete Aggregates (RCA). Twelve slabs were tested, employing three different span lengths, currently used in practice, (2.4 m, 2.8 m, and 3.2 m) and four mix designs with varying RCA replacement percentages (0 %, 30 %, 50 %, and 100 %). The slabs were subjected to four-point bending tests to determine their load-bearing capacity and interface bond strength. The presence of RCA seems to enhance longitudinal shear strength, which confirms its suitability in sustainable construction suggesting that it is actually right to follow the path herein outlined.

1. Introduction

Concrete, a ubiquitous construction material, presents multifaceted environmental challenges. Its production, primarily reliant on cement, contributes significantly to carbon dioxide emissions [1,2], exacerbating climate change. The extraction of raw materials for concrete, including sand (fine aggregate) and gravel (coarse aggregate), unfortunately leads to habitat disruption and resource depletion [3], impacting biodiversity and ecosystems. The water-intensive nature of concrete production, coupled with improper waste disposal from construction and demolition activities, poses risks to water resources and amplifies the global waste stream. Concrete high thermal conductivity contributes to the urban heat island effect, altering local climates, while its reflective properties influence the albedo effect, potentially impacting regional climate patterns. Improper disposal of concrete-related chemicals can lead to groundwater contamination, posing risks to both human health and aquatic ecosystems. Construction and demolition processes, see [4], generate airborne concrete dust with adverse respiratory effects on humans and surrounding ecosystems. Furthermore, the long lifespan and inflexibility of concrete structures inhibit adaptive responses to changing environmental needs and conditions, emphasizing the need for sustainable alternatives and responsible construction practices.

Recycled Concrete Aggregate (RCA) emerges as a very promising solution to mitigate the depletion of natural resources induced by traditional concrete construction [5]. By utilizing RCA in concrete production, the demand for fresh aggregates extracted from quarries can be remarkably reduced, thereby preserving natural ecosystems and mitigating habitat disruption. This practice not only extends the lifespan of existing resources but also minimizes the environmental impact associated with extraction processes [6]. Recycling concrete not only diverts waste from landfills but also lessens the need for virgin materials, addressing the sustainability challenges posed by resource depletion. Consequently, the incorporation of RCA in concrete promotes a more circular and environmentally conscious approach to construction,

* Corresponding author.
E-mail address: fstochino@unica.it (F. Stochino).

https://doi.org/10.1016/j.istruc.2024.107838
Received 31 July 2024; Received in revised form 27 October 2024; Accepted 11 November 2024
Available online 16 November 2024

contributing to the conservation of natural resources and fostering a more sustainable built environment.

The mechanical performance of recycled aggregate concrete is being thoroughly investigated [7]. Previous studies on RCA report on reduced compressive strength but enhanced interfacial bonding due to rougher surfaces [8]. Recently, it has been investigated the fracture behavior of environmentally-friendly building materials such as rubberized steel fiber reinforced recycled aggregate concrete (RSRAC), which incorporates waste concrete and tires [9]. Very promising results indicate that RSRAC exhibits reduced brittleness and improved ductility with crumb rubber, while steel fiber enhances strength but increases brittleness, and recycled aggregate negatively affects both strength and ductility.

From this perspective, the composite concrete-steel solutions (Fig. 1), like slabs, can provide interesting research results, see [10,11]. Composite steel concrete slabs combining steel and concrete, offer a synergistic effect by leveraging the tensile strength of steel and the compressive strength of concrete, resulting in enhanced structural performance and durability. These systems are particularly advantageous in construction, providing increased load-bearing capacity and efficient material usage.

The response of such structures is governed by the tangential behaviour of the interface, i.e. the bond between the two materials, and for this reason the roughness of the concrete became more important than its ultimate strength [12,13]. The longitudinal shear strength ($\tau_{u,Rd}$) stress, which governs the design of a composite slab, can be assessed by using the interaction domain proposed by the EN1994-1-1 [14], together with the experimental results of a four point bending test procedure, i.e. by following the so-called partial shear connection (PSC) method. The main assumptions of the method are: i) at the ultimate limit state, the steel sheet response is always in the plastic range independently of the effective strain value reached at the various levels of the cross-section; ii) the contribution of the concrete inside the ribs is always neglected.

These simplified assumptions affect the resistance domain and could leads to a non-reliable estimation of the level of interaction between concrete and steel. As already observed in Ref. [15], it can be noted that once a limit strain ε_{lim} of the lower edge of the steel deck is reached, longitudinal shear collapse occurs, with a large part of the steel deck in the elastic range. For this reason more refined design method are still under investigation [16].

Therefore, it is clear that to reach satisfactory level of resistance and stiffness, it is not necessary to use high-resistant concrete but is really important to guarantee an high mechanical and chemical interlock with the steel sheeting. In this view, concrete made with recycled aggregates seems to be a perfect solution.

To investigate the response of composite slabs with recycled concrete the Italian Ministry funded the SARCOS project [17], based on a strict collaboration between the University of Cagliari and the Politecnico di Milano.

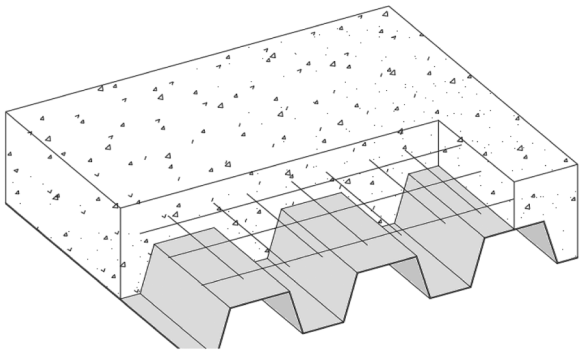

Fig. 1. Typical steel-concrete slab with trapezoidal metal deck.

The primary aim of this research is to evaluate the mechanical behavior of composite concrete-steel slabs incorporating recycled concrete aggregates (RCA). Specifically, this paper reports on the preliminary experimental campaign has been executed by testing 12 slabs at the *Materials Testing Laboratory* at the University of Cagliari: 4 concrete mixes, characterized by different recycled aggregates replacement percentage from 0 % to 100 %, have been used and they were respectively labelled as M0-0, M30-30, M50-50, M100-100. For each mix, 3 different span lengths have been considered: 2400, 2800 and 3200 mm. Ultimate resistance and longitudinal shear resistance of the slabs are presented and discussed in function of the percentage of recycled aggregates.

After this brief introduction, the paper is organized as follows: the adopted materials are presented in Section 2, while the testing campaign and the main associated research outcomes are described in Section 3. The estimation of the longitudinal shear strength is reported in Section 4 while conclusive remarks are finally discussed in Section 5.

2. Tests on materials

2.1. Concrete

For the construction of the slabs, TECNOCEM A-LL 42.5 R, a Portland limestone cement type II with chemical requirements (Sulphates (as SO3) $\leq$ 4.0 %, Chloride $\leq$ 0.10 %), was used for this research. Table 1 presents the characteristics of the aggregates used. Additionally, a superplasticizer additive was adopted in all mixes. Potable water, without any additives and at a temperature according to ASTM C1602 [18], was used in the production of the mix designs. The fine and coarse recycled aggregates was obtained from the demolition waste of a RC building in Cagliari.

Four mix designs (M) were considered to investigate the effect of replacing recycled aggregates with natural aggregates. The characteristics of these designs are listed in Table 2. In the mix designs notations, the first number indicates the replacement percentage of fine natural aggregates with fine recycled concrete aggregates, and the second number represents the replacement percentage of coarse natural aggregates with coarse recycled concrete aggregates. A constant water-to-cement ratio of 0.51 was maintained across all mix designs. It is important to point out that the recycled aggregates absorbed more water during mixing than natural aggregates. For this reason, all the aggregates were pre-saturated before mixing and only the effective water available for the cement was the same for each mix. As a consequence, the total water changes accordingly to the amount of recycled aggregates present in each mix. Fig. 2 presents the granulometry curves for the aggregates used in each mix, showing the particle size distribution for the natural and recycled aggregates. This comparison illustrates the differences in gradation among the mixes, which influence the mechanical properties and workability of the concrete.

At the same time as the composite slabs were casted, cubic samples were also prepared using 150 × 150 × 150 mm cube molds for mechanical tests. The cubic and composite slab samples were kept in standard laboratory conditions for 24 h (at a temperature of 23 ± 2 °C) and then removed from the molds. Subsequently, the samples were cured by being wrapped in plastic covers. The cube samples underwent

Table 1
Specifications of the aggregates.

Component	Max size aggreg. [mm]	Wat. absorption [%]	Dry density [kg/m^3]
Coarse Natural	12.5	0.9	2690
Fine Natural	5.0	1.5	2830
Coarse Recycled	12.5	6.4	2460
Fine Recycled	5.0	12.9	2240

Table 2
Mixtures compositions.

Mix	Cement [kg/m^3]	Water/Cement	Fine VA/Fine RA	Coarse VA/Coarse RA
M 0-0	366	0.51	0	0
M 30-30	366	0.51	30	30
M 50-50	366	0.51	50	50
M 100-100	366	0.51	100	100

curing for 7, 28, and 90 days, while the composite slabs were cured for 28 days.

The compressive strength of cubic samples at 7, 28, and 90 days was measured in accordance with EN 12390-3 [19]. The compression load was applied by means of a hydraulic press machine (manufactured by Controls Testing Equipments Ltd) with a capacity of 3000 KN and a digital force control. The load was applied with a constant rate of 0.4 MPa/s till the specimen collapse.

Additionally, a 28-day splitting test was conducted, according to the standards outlined in EN 12390-6 [20]. In this case, the same load-controlled machine was used, along with a suitable steel frame design, to subject the concrete cubes to a splitting tensile test at a constant load rate of 0.04 MPa/s. The impact of replacing recycled concrete aggregates on the compressive strength of cube concrete samples at 7 and 90 days is presented in Fig. 3. Furthermore, Fig. 4 depicts the results obtained from the compression and the tensile test after 28 days. The M0-0 mix, which contains 0 % RCA, exhibited a 28-day compressive strength of 43 MPa. This value is consistent with the performance of C30/37 concrete, in accordance with EN 206 [21] standard, which is commonly used in composite slab applications. The compliance with industry standards ensures that the control specimen provides a reliable baseline for comparing the effects of RCA on the mechanical properties of composite slabs.

The presented results indicate that an increase in the replacement of recycled concrete aggregates leads to a reduction in the compressive strength at 7, 28, and 90 days, as well as the tensile strength at 28 days. Specifically, for the M100-100 mix design with complete replacement of fine and coarse recycled concrete aggregates, as compared to the M 0-0 mix design with natural aggregate, there is a decrease in compressive strength of approximately 17 MPa for the 90-day compressive

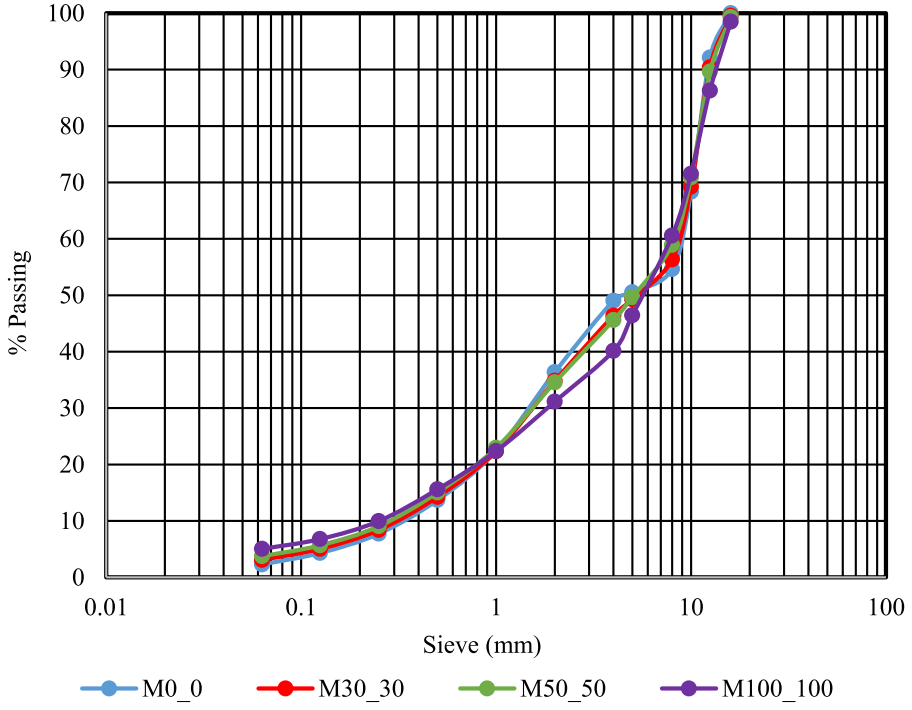

Fig. 2. Aggregates granulometry curves for each mix.

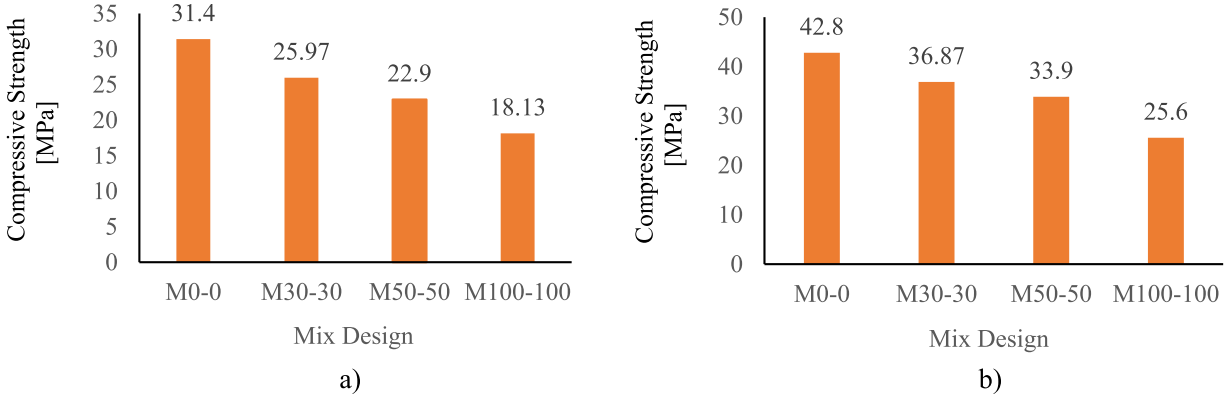

Fig. 3. Effect of recycled concrete aggregates replacement on compressive strength: a) 7 days, b) 90 days.

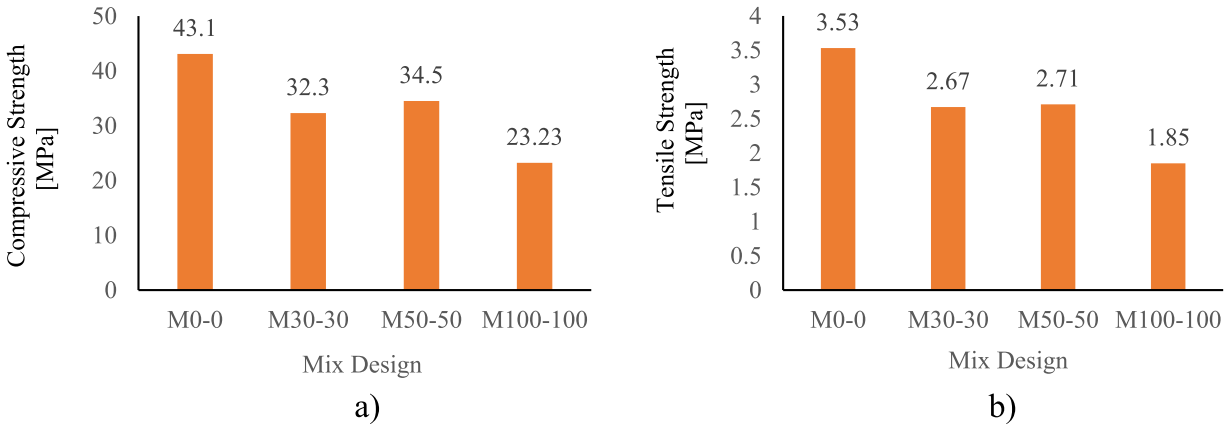

Fig. 4. Effect of recycled concrete aggregates replacement after 28 days of curing: a) compressive and b) tensile strength.

strength. This phenomenon can be attributed to the weaker nature of the recycled concrete aggregates in the interfacial transition zone (ITZ) compared to natural aggregate. The presence of mortar adhered to the recycled aggregate contributes to this weakness.

The Modulus of Elasticity in compression was determined in accordance with UNI-EN 12390-13: 2013 [22]. For each concrete type, two cylindrical specimens with diameters of 150 mm and heights of 300 mm were fabricated and subjected to testing. Table 3 illustrates the average results and coefficient of variation (CoV) for each test.

The M 0-0 mix, which lacked recycled content, exhibited the highest average Modulus of Elasticity at 34.7 GPa, albeit with a relatively high coefficient of variation (CoV) of 13.43 %. Conversely, mixes incorporating recycled aggregates (M30-30, M50-50, and M100-100) demonstrated more consistent properties, as evidenced by their lower CoVs of 0.53 %, 1.45 %, and an exceptionally small 0.03 %, respectively. As indicated in Table 3, there is a clear trend showing that an increase in the replacement percentage decreases the elastic modulus value of concrete, aligning with expectations and findings from existing literature [23]. Hence, it is expected that the higher the percentage of aggregate replacement, the greater the deformability of the slab.

2.2. Steel sheeting

The steel material for the sheeting is a S280GD used for cold-formed profiles. The deck has been provided by Spinelli srl, named SG110-600, which is a special deck having a total height of the ribs equal to about 110 mm, which is not usual for this type of profile (Fig. 5). The thickness of the sheeting is constant and equal to 0.75 mm. It has been used the same identical profile for all the tested slabs. Tensile tests on four coupon samples identified a mean yielding tension equal to 338.18 MPa and a mean ultimate tension equal to 593.16 MPa. The mean value of the Young Modulus is equal to 195 GPa.

3. Testing campaign

3.1. Test description

Experimental tests were performed employing a loading machine outfitted with a hydraulic jack, facilitating precise loading on all slabs at two predetermined points at L/4 from midspan, where L denotes the span length of the slab. All the specimens were restrained with a simple support and an hinge at their ends. The displacement of the slabs was monitored at 8 distinct locations using linear displacement transducers (LVDTs) with a nominal displacement of 100 mm, nominal sensitivity 2 mV/V, sensitivity tolerance ± 0.1 %, measure resolution 1 μm. In particular, 4 LVDTs were used to monitor the debonding of the slab, i.e. the lateral relative deformation between the steel and the concrete. The instrument position and the static scheme of the tests is reported in Fig. 6.

The loading protocol involved two successive load cycles up to 30 % and 50 % of the theoretical collapse load, respectively. After these load cycles in the testing sequence, a third loading cycle was performed until reaching the peak load, corresponding to the debonding failure of each slab specimen. This kind of failure occurs when the bond between the concrete and the steel is compromised. Following this peak measurement, the slabs were subjected to additional loading until flexural failure that occurred at a lower load. This behavior was detected for each slab specimen showing an intrinsic *ductility* for this kind of structure.

Table 3
Concrete modulus of elasticity.

Mix	Average [GPa]	CoV (%)
M 0-0	34.7	13.43
M 30-30	22.5	0.53
M 50-50	23.7	1.45
M 100-100	16.7	0.03

3.2. Load versus vertical displacement

The applied vertical load is plotted in Figs. 7–9 as a function of the middle displacement (M and L transducers, see Fig. 6 for their positions). Figures differ for the length of the slab, while the different mix design are grouped together in the same figure. This representation allows for a comprehensive understanding of how varying structural dimensions influence the response to the test. It can be noted that, for the 2400 mm span, the M 30-30 mix design demonstrated the highest vertical load while for the 2800 mm and 3200 mm spans, the maximum vertical load is associated with the M 50-50 and the M 100-100 mix design, respectively.

Some patterns are common for all Figs. 7–9: the initial linear portion is influenced by the elastic response of both materials, whereas post-peak behavior shows debonding and subsequent flexural deformation. The sudden drop in load post-peak is explained as a debonding failure, followed by a ductile phase characterized by progressive cracking and load redistribution.

The collapse mechanism exhibited uniformity across all slabs: upon reaching the maximum load, debonding initiates (as depicted in Fig. 10), resulting in a sudden decline in the curves. This initial debonding phase is succeeded by a flexural mechanism, inducing substantial deformations despite minimal load variation. With the progression of cracking, the bond between the concrete and steel further deteriorates, facilitating the expansion of the debonded region. Ultimately, this enlarged debonded area compromises the structural integrity of the composite slab. Following debonding, a flexural mechanism ensues, redistributing loads within both the composite slab and its supporting

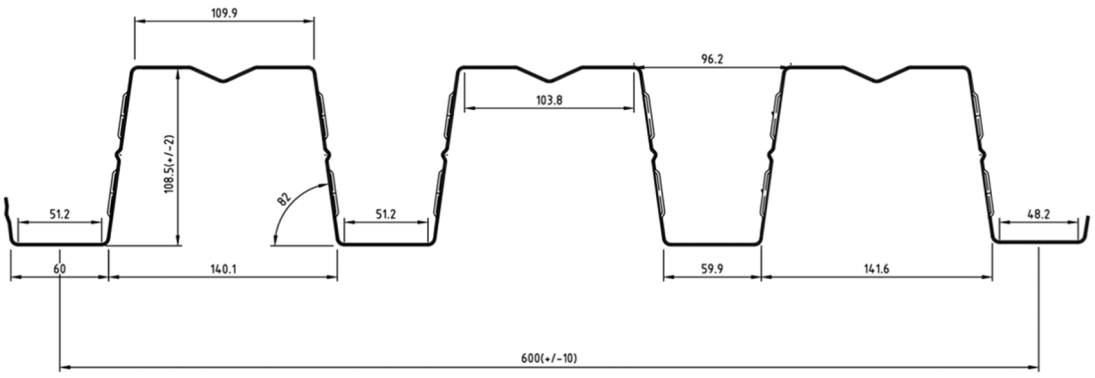

Fig. 5. Steel sheet geometric characteristics from Spinelli srl, (named SG110-600), measures in mm.

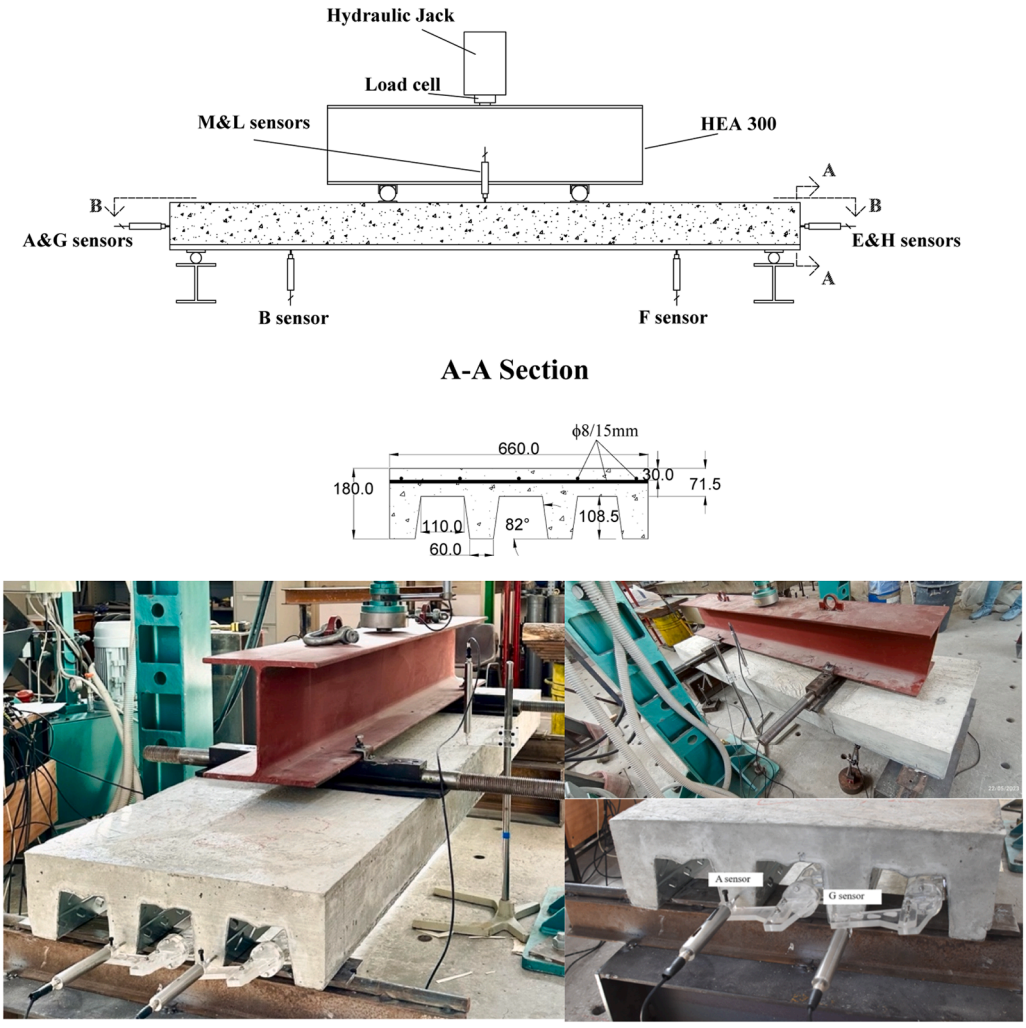

Fig. 6. Experimental set-up of the composite slab test. Top: drawings and sensors location, bottom: pictures from the experimental tests.

structure. Once debonding transpires, the composite slab forfeits its complete composite action, necessitating load redistribution. While the remaining bonded sections continue to support a fraction of the loads, the distribution becomes uneven. Regions proximate to the debonded area undergo heightened stresses as they bear a larger portion of the load, potentially leading to localized overstressing and subsequent failure if unaddressed. The severity of debonding and the capacity of the remaining bonded areas determine whether the composite slab experiences flexural failure in localized regions, as illustrated in Fig. 11. This failure mode can manifest through cracking, excessive deflection, or in extreme scenarios, complete collapse.

The collapse load at the center of all composite slabs is provided in Table 4. Referring to Table 4, it can be noted that the increment in the percentage of recycled aggregate also corresponds to a load increment which is contrary to the previous results related to the mechanical properties of the mix designs. This implies that an increase in the replacement of recycled aggregates in composite slabs results in an enhancement of bonding strength. Augmenting the replacement of

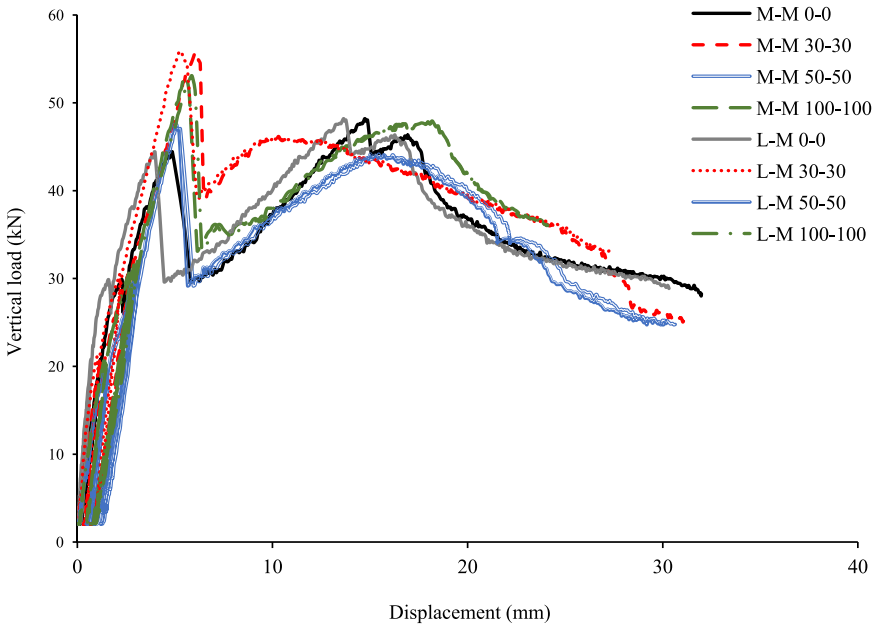

Fig. 7. Load-displacement curves (M and L, LVTD) for 2400 mm span.

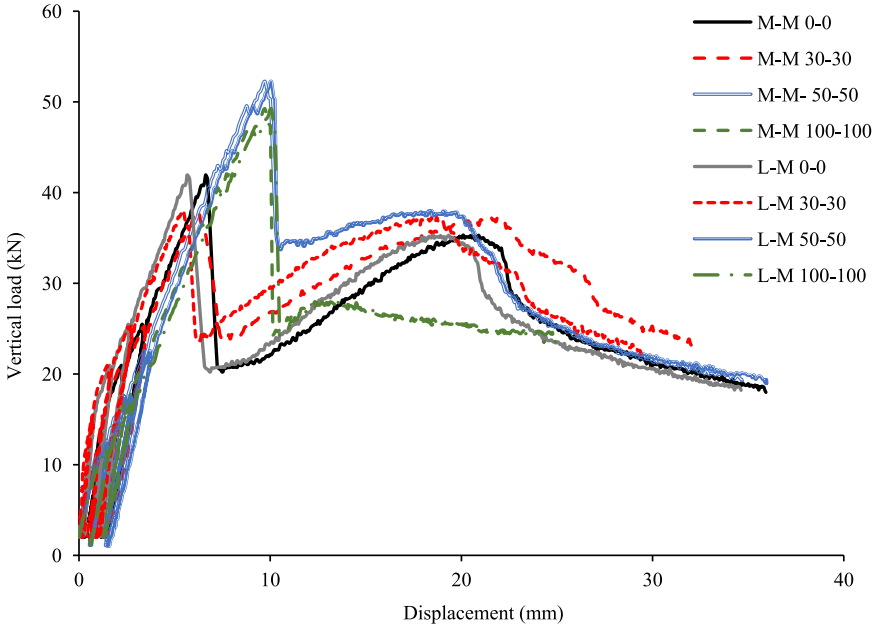

Fig. 8. Load-displacement curves (M and L, LVTD) for 2800 mm span.

recycled concrete aggregates has heightened the friction between concrete and steel sheets, i.e. increasing the longitudinal shear strength. These results are in agreement to those presented in [23-25] and suggest that the use of recycled aggregates, with a focus on reducing environmental impacts and promoting a circular economy, can lead to improved structural performance in composite slabs and mechanical systems where bonding is critical.

3.3. *Load versus horizontal displacement*

As previously discussed at the peak load the debonding is detected and the relative displacement between the sheeting and concrete occur. This relative displacement has been monitored by the use of E&H and G&A LVDTs. The output from these transducers have been plotted in Figs. 12–14. It is important to note that, for clarity, only the most significant results are shown. Therefore, not all transducers are represented in every figure.

It can be noted that until the debonding load is not reached the lateral displacement is almost equal to zero. At this load level the slab starts to deform laterally. These graphs confirm that the load level assumed as the debonding load is really associated with this lateral slippage of the slab. The position of the first movement seems to be quite casual, depending on imperfections of the slab and of the load and supports positions. For this reason, is not easy also to find a rule to describe how the maximum displacement is influenced by the recycled aggregate percentage.

4. Estimation of the longitudinal shear strength

Starting from the experimental results, the degree of interaction (η)

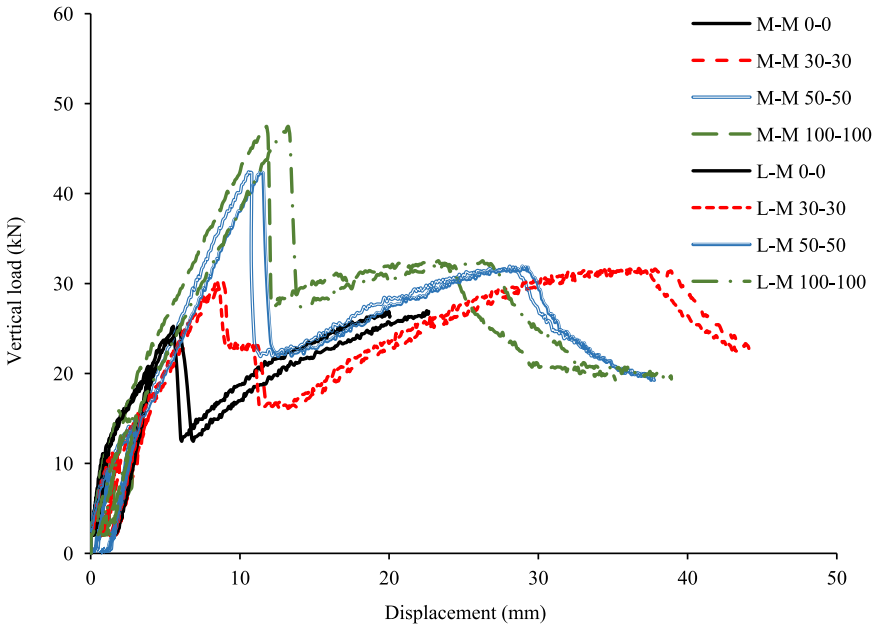

Fig. 9. Load-displacement curves (M and L, LVTD) for 3200 mm span.

Fig. 10. Typical relative displacements of the steel sheet with respect the concrete during the test.

Fig. 11. Flexural crack at the end of the test.

Table 4
Collapse load [kN] of the tested slabs.

Mix design	2400 mm	2800 mm	3200 mm
M 0-0	48.20	41.96	26.98
M 30-30	55.91	38.01	31.67
M 50-50	47.53	52.24	42.41
M 100-100	53.05	49.23	47.45

and then the longitudinal shear strength (τ_u) was evaluated by means of the use of the partial interaction domain (PSC) of the EC4-1-1 [14]. The main hypotheses of the procedure are: i) at the ultimate limit state (ULS) the thin steel deck works always in plastic range independently on the stress level reached in the cross-section. The position of the plastic axis of the steel sheet is identified by terms e_p; ii) the concrete inside the ribs gives no contribution to the final resistance; iii) when the degree of interaction is equal to zero ($\eta = 0$), only the effective bending resistance of the steel sheeting is considered. The effective properties of the steel hi-bond under pure bending were evaluated following the prescriptions of EC3-1-3 [26] by properly considering the presence of stiffeners on the cross-section which produce also distortional buckling in addition to the local one. The obtained effective section is plotted in Fig. 15.

The maximum compression, which is assumed to act on the concrete, N_{cf}, is equal to (Fig. 16):

$$N_{cf} = b \bullet h_c \bullet 0.85 f_{cm} \quad (1)$$

where b is the width of the section, h_c is the height of the concrete slab above the steel sheeting and f_{cm} is the mean value of the cylindrical resistance of the concrete. It can be observed that the interaction domain is influenced by the mechanical properties of the concrete, for this reason we will obtain one different domain for each mix design.

From the equilibrium between the maximum compression on the concrete and the maximum tension on the steel, it is possible to evaluate

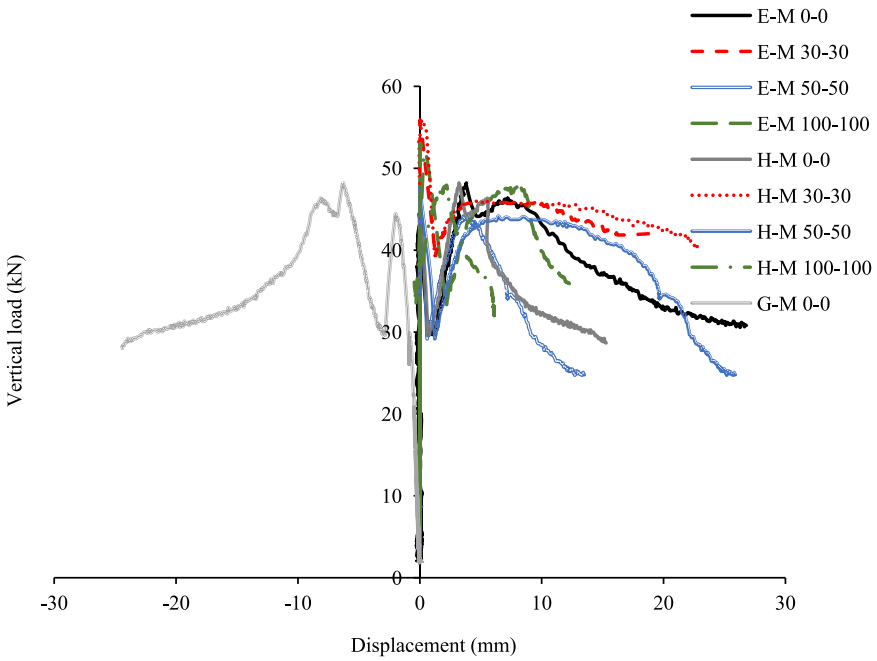

Fig. 12. E&H&G and A sensors displacement versus the load, 2400 mm slab.

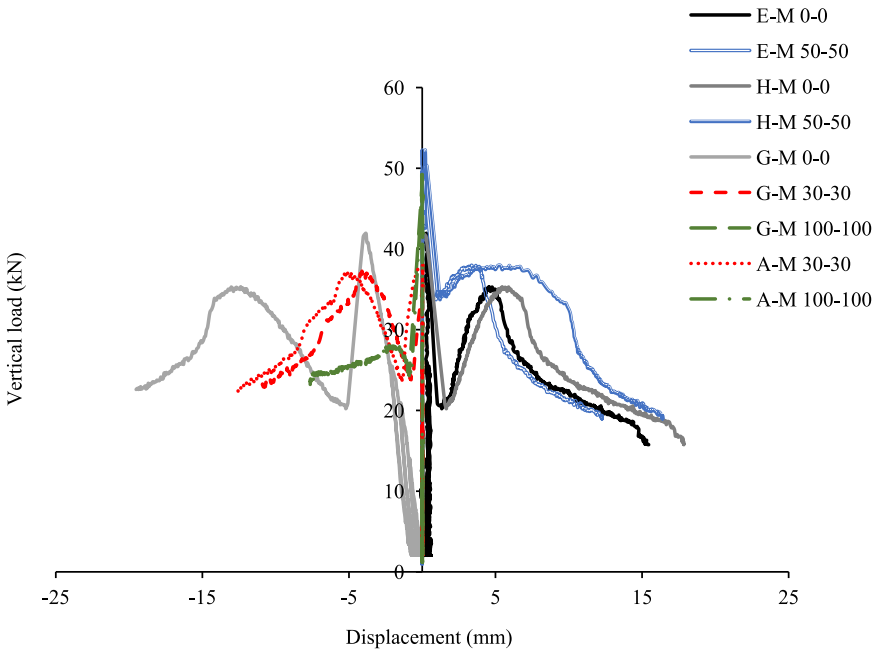

Fig. 13. E&H&G and A sensors displacement versus the load, 2800 mm slab.

the position of the neutral axis, x:

$$A_p \quad f_{yp} = 0.85 \quad f_{cm} b \quad x; x = \frac{A_p \quad f_{yp}}{0.85 \quad f_{cm} \quad b} \tag{2a,b}$$

where A_p is the area of the steel sheeting and f_{yp} is the correspondent yielding, experimentally assessed.

For the partial interaction (i.e., $0 < \eta < 1$) the position of the neutral axis depends on the grade of interaction, $x' = \eta\, x$. It can be noted that when the grade of interaction is nil, the neutral axis coincides with the top axis of the section. As a consequence, also the force on the compressed part decreases with the decrement of η, $N_c = \eta\, N_{cf}$.

The bending resistance is then obtained considering the equilibrium to the rotation with respect to the neutral axis, ranging from the maximum value, $M/M_{p,Rm}$, obtained with $\eta = 1$ to the minimum one, i.e. the bending resistance of the steel sheeting. The non-dimensional M- η domain obtained from M0-0 slab is proposed in Fig. 17 which can be assumed as significant for each mix design.

The value of the degree of interaction is obtained by entering with the experimental bending moment M_{test} into the domain (Fig. 18).

Finally, the longitudinal shear strength, τ_u, is directly obtained from equation:

$$\tau_u = \frac{\eta N_{cf}}{b \quad l_s} \tag{3}$$

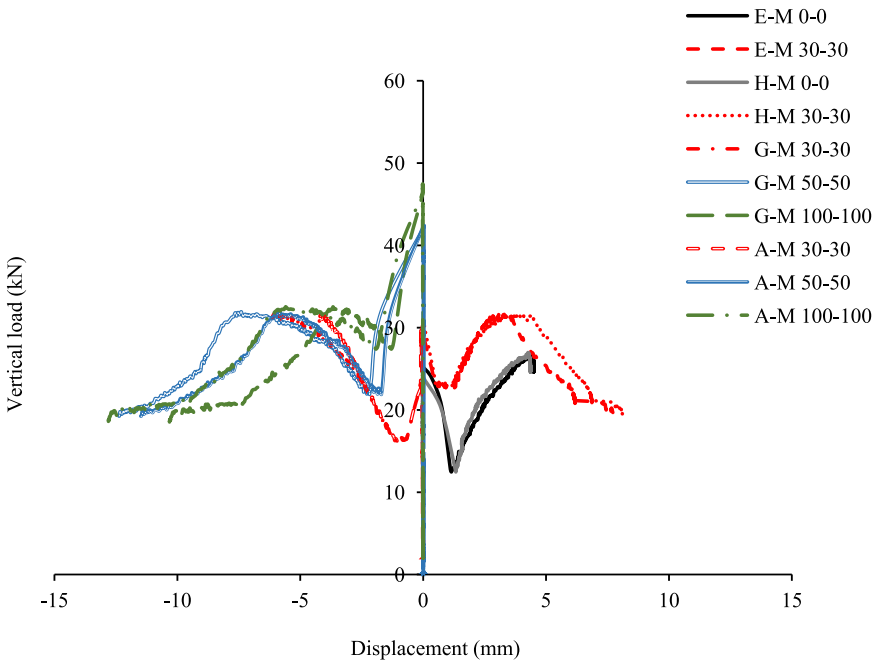

Fig. 14. E&H&G and A sensors displacement versus the load, 3200 mm slab.

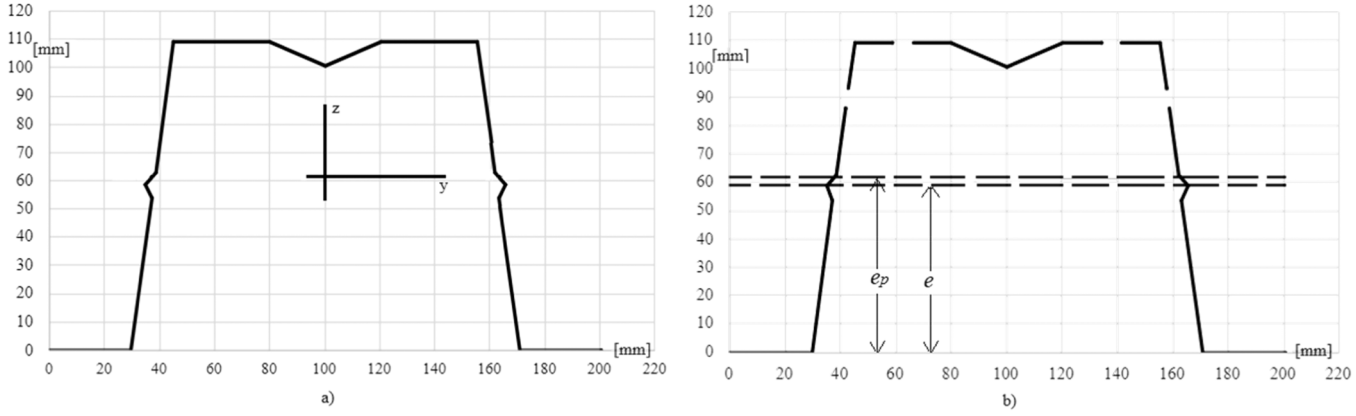

Fig. 15. Gross (a) and effective (b) cross-section of the metal deck in bending.

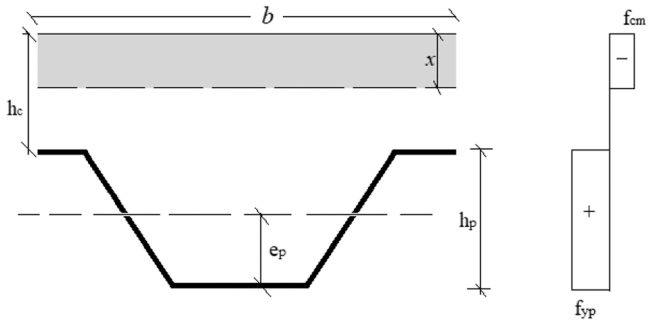

Fig. 16. Stresses distribution on the composite section.

where l_s is the distance between the force and the support, equal to L/4.

The ratio between the longitudinal shear stress obtained from each slab, over the M0-0 mix design, i.e. $\tau_{u,i}/\tau_{u,M0}$, is reported in Table 5. The average value between each length and the covariation is reported too.

It is confirmed that the use of concrete made by recycled aggregates brings a non-negligible improvement in term of longitudinal adhesion between the two materials, the longitudinal shear is increased, in mean, up to 1.7 times.

The increased bond strength between RCA concrete and steel sheeting can be attributed to the enhanced roughness of RCA surfaces. The adhered mortar on recycled aggregates increases the friction coefficient and results in better mechanical interlock with the steel deck. We referenced studies (e.g., [23]) that report similar observations.

5. Conclusions

This study presents initial findings from research investigating the flexural characteristics of composite steel-concrete slabs made of concrete containing recycled aggregates. The investigation illustrates that integrating recycled aggregates into composite slab construction represents a current [26,27] and feasible approach to mitigating environmental impact while maintaining high structural performance. Utilizing recycled aggregates up to a specified threshold emerges as a practical alternative to conventional natural aggregates, thereby aligning with principles of sustainable construction.

The analysis of collapse load data indicates that composite slabs incorporating recycled content can exhibit either improved or similar

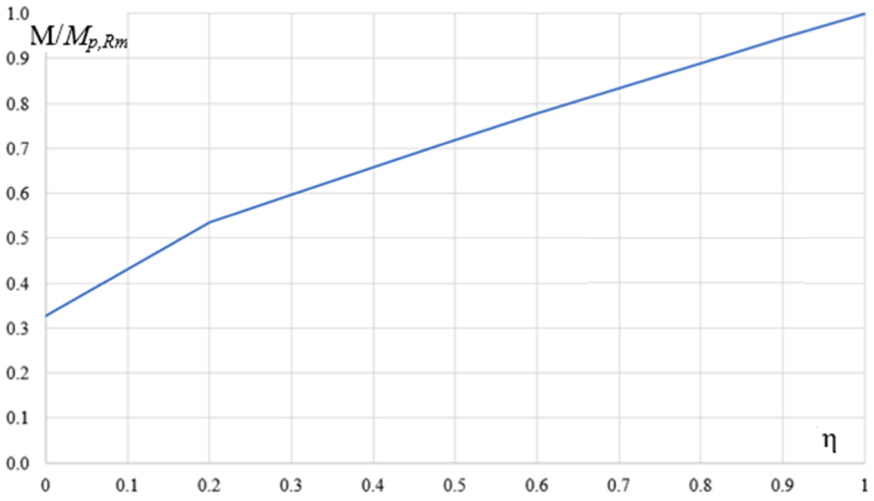

Fig. 17. The M- η domain for the composite section with M0-0 mix design.

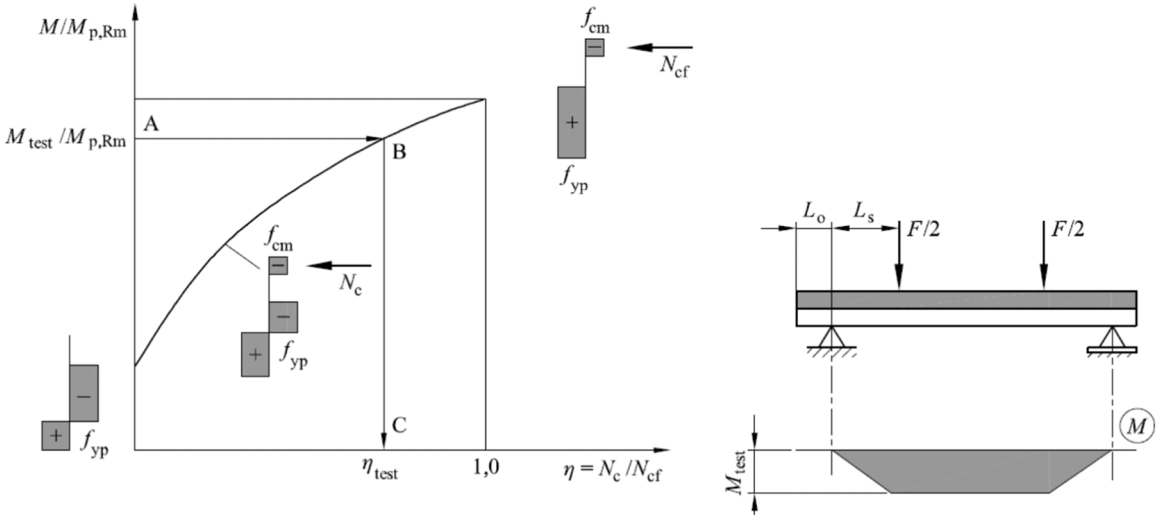

Fig. 18. Approach for the determination of the degree of interaction (EC4).

Table 5
Non-dimensional longitudinal shear strength.

	2400 mm	2800 mm	3200 mm	average	CoV (%)
$\tau_{u,M30}/\tau_{u,M0}$	1.59	0.70	0.64	0.98	0.19
$\tau_{u,M50}/\tau_{u,M0}$	0.95	1.92	1.47	1.44	0.15
$\tau_{u,M100}/\tau_{u,M0}$	1.30	1.57	2.14	1.68	0.13

load-bearing capacities compared to traditional concrete slabs, particularly under specific span lengths. These preliminary findings challenge conventional assumptions that recycled aggregates inherently result in diminished structural performance, underscoring the potential for tailored recycled aggregate proportions to achieve desired strength characteristics in particular for composite structures [28].

The ductile behavior observed in composite slabs with recycled aggregates is confirmed from the extensive experimentally observed deformation and the ability of the slabs to sustain loads post-debonding, suggesting a high potential for energy dissipation, particularly useful in seismic regions. The enhanced bond strength between the recycled aggregate concrete and steel sheeting suggests a promising avenue for further optimization of composite slab designs.

The use of recycled aggregates has shown structural benefits, such as improved bonding with steel sheets, which enhances the overall performance of composite slabs.

However, the research emphasizes the imperative for further investigation to optimize mix designs, assess the long-term performance of recycled aggregate slabs, and ascertain their applicability across diverse structural contexts. Future studies should explore long-term performance of RCA-based composite slabs, particularly focusing on creep and fatigue behavior, effects of freeze-thaw cycles and moisture exposure, but also on thermal properties of recycled aggregate composite slabs to provide a comprehensive understanding of their performance over the lifecycle of a structure.

In essence, this study underscores the significant role recycled aggregates can play in fostering sustainable construction practices while ensuring the preservation of mechanical performance in composite slab design through meticulous consideration of material properties. By continuing to refine and expand upon these initial findings, the construction industry can move closer to achieving its sustainability goals without compromising structural integrity.

CRediT authorship contribution statement

Marco Andrea Pisani: Validation, Supervision, Conceptualization. **Marco Simoncelli:** Writing – original draft, Validation, Supervision, Funding acquisition, Formal analysis, Conceptualization. **Giovanna**

Concu: Validation, Supervision, Conceptualization. **Monica Valdes:** Methodology, Investigation, Data curation. **Claudio Bernuzzi:** Validation, Supervision, Formal analysis, Conceptualization. **Marco Zucca:** Writing – review & editing, Validation, Investigation, Conceptualization. **Alireza Alibeigibeni:** Writing – original draft, Methodology, Investigation, Data curation. **Flavio Stochino:** Writing – original draft, Supervision, Resources, Project administration, Methodology, Investigation, Funding acquisition, Conceptualization.

Conflict of Interest

The authors declare no conflict of interest for the manuscript entitled "Mechanical Behavior of Composite Slabs with Recycled Concrete Aggregates: A Preliminary Study".

Acknowledgement

The financial support of project SARCOS PRIN2022 – CUP: F53D23002030006 - Prot. 2022WWN3TC is acknowledged. The authors extend their sincerest thanks to the Spinelli srl Company for providing the steel sheets (named SG110-600) essential for this research.

References

[1] Broyles JM, Hopper MW. Assessment of the embodied carbon performance of post-tensioned voided concrete plates as a sustainable floor solution in multi-story buildings. Eng Struct 2023;295:116847.
[2] Mak MWT, Lees JM. Carbon reduction and strength enhancement in functionally graded reinforced concrete beams. Eng Struct 2023;277:115358.
[3] Habert G, Bouzidi Y, Chen C, Jullien A. Development of a depletion indicator for natural resources used in concrete. Resour Conserv Recycl 2010;54(6):364–76.
[4] Yang J, Wu Y, Zhou G, Xin G. The dismantling method of wheel-spoke cable-strut tension structures based on experimental and numerical study. Structures 2023;48:1949–63.
[5] Zhang Huan, et al. Experimental study and prediction model for bond behaviour of steel-recycled aggregate concrete composite slabs. J Build Eng 2022;53:104585.
[6] Zhang H, Geng Y, Wang YY, Wang Q. Long-term behavior of continuous composite slabs made with 100 % fine and coarse recycled aggregate. Eng Struct 2020;212:110464.
[7] Wang D, Lu C, Zhu Z, Zhang Z, Liu S, Ji Y, et al. Mechanical performance of recycled aggregate concrete in green civil engineering. Case Stud Constr Mater 2023;19:e02384.
[8] Liu Y, Zhou J, Zhao T, Sun H, Kang T, Li S, et al. Bond behavior of recycled-fiber recycled concrete and reinforcement. J Mater Civ Eng 2023;35(5):04023093.
[9] Xu J, Chang F, Bai J, Liu C. Statistical analysis on the fracture behavior of rubberized steel fiber reinforced recycled aggregate concrete based on acoustic emission. J Mater Res Technol 2023;24:8997–9014.
[10] John K, Ashraf M, Weiss M, Al-Ameri R. Experimental study and numerical modelling of a novel two-way steel-concrete composite slab. Structures 2023;57:105096.
[11] Loureiro MC, Alves ÉC, Calenzani AFG. Geometry optimization of steel formwork for steel–concrete composite slabs. Structures 2023;58:105395.
[12] Zhang H, Zhang HY, Geng Y, Fang PQ, Wang YY. Design formulae for long-term responses of continuous steel-recycled aggregate concrete composite slabs. Structures 2022;45:1477–90.
[13] Ranzi G, Leoni G, Zandonini R. State of the art on the time-dependent behaviour of composite steel–concrete structures. J Constr Steel Res 2013;80:252–63.
[14] CEN EN1994-1-1. Eurocode 4: design of composite steel and concrete structures – Part 1-1-: general rules and rules for buildings; 2004.
[15] Bernuzzi C, Pisani MA, Simoncelli M. Debonding strain for steel-concrete composite slabs with trapezoidal deck. Steel Compos Struct 2023;49(1):19–30.
[16] Hedaoo NA, Gupta LM, Ronghe GN. Design of composite slabs with profiled steel decking: a comparison between experimental and analytical studies. J Adv Struct Eng 2012;3:1–15.
[17] SARCOS project website: ⟨https://projectsarcos.it/⟩ [accessed 2024].
[18] ASTM C1602. Standard specification for mixing water used in the production of hydraulic cement concrete. ASTM international; 2018.
[19] CEN EN12390-3. Testing hardened concrete – Part 3: compressive strength of tests specimens; 2019.
[20] EN 12390-6. Testing hardened concrete – Part 6: tensile splitting strength of test specimens; 2023.
[21] EN 206:2013 concrete – specification, performance, production and conformity.
[22] CEN EN12390-13. Testing hardened concrete – Part 13: determination of secant modulus of elasticity in compression; 2021.
[23] Wang D, Lu C, Zhu Z, Zhang Z, Liu S, Ji Y, et al. Mechanical performance of recycled aggregate concrete in green civil engineering. Case Stud Constr Mater 2023;19:e02384.
[24] Butler LJ, West JS, Tighe SL. Bond of reinforcement in concrete incorporating recycled concrete aggregates. J Struct Eng 2015;141(3):B4014001.
[25] Sirico A , Palii O, Pappalardo M, Plaza P, Sanchez, J, Bernardi P, et al. Investigating bond strength and performance of reinforced concrete with recycled aggregates. In: Proceedings of the Italian concrete conference. Florence; 2024.
[26] CEN EN1993-1-3. Eurocode 3: design of steel structures – Part 1-3-: general rules – supplementary rules for cold-formed members and sheeting; 2006.
[27] Liu Z, Zhao YG, Ma L, Lin S. Review on high-strength recycled aggregate concrete: mix design, properties, models and structural behaviour. Structures 2024;64:106598.
[28] Jin J, Ming W, Jian L, Pengcheng Z. Study of recycled aggregate concrete-filled circular steel columns with H-shaped steel reinforcement. Structures 2023;55:1960–5.